Demonstration of self-spiking neuron behavior in a monolithically integrated two-section laser

Lukas Puts[1], Kevin Williams[1], Daan Lenstra[1] and Weiming Yao[1]

[1]Photonic Integration Group, department of Electrical Engineering,
Eindhoven University of Technology, P.O. Box 513, Eindhoven 5600MB, The Netherlands
[*]l.puts@tue.nl

An integrated two-section laser with saturable absorber and gain section fabricated in an InP technology platform is analysed. Bistability and a voltage depending self-spiking behaviour are demonstrated. Additional simulations show that the self-spiking behaviour is likely triggered by noise, and that the pulse density can be controlled by the absorber voltage. This makes the proposed device a most promising encoder in a photonic spiking neural network.

Keywords: *optical neuron, spiking neuron, bistable laser, photonic integrated laser*

INTRODUCTION

Due to the development of novel artificial intelligence (AI) algorithms and neural network modelling, big data and the predictions of the end of Moore's Law, research into AI has grown exponentially [1]. The efficiency and speed of large neural networks in conventional hardware is limited due to the Von Neumann bottleneck, and thus new ways to implement neural networks in hardware are being explored [2]. One specific type of neural network is a spiking neural network (SNN), which comprises artificial neurons in multiple layers that closely mimic the dynamics of its biological counterpart, and thus attracted significant research interest. In an SNN, input data can be encoded using a temporal based or a rate based encoding scheme. In the latter, the input data is translated to a density of pulses at the input layer [3]. After this input layer, very short pulses are generated by individual neurons and transmitted as an optical trigger to consecutive neurons. The next neuron then either fires a spike or remains in its rest state. In an all-optical photonic spiking neuron (PSN), these optical spikes can potentially be very fast and short in time, and consequently an SNN based on photonic components can offer high operational speed at potentially low power consumption. To achieve this, various strategies to attain a photonic spiking neuron were recently proposed. For example, an integrated optical neuron based on a VCSEL [4] or a fiber laser [5] have been investigated. However, a fully integrated and scalable excitable spiking neuron for spike processing and data encoding has not yet been demonstrated.

A saturable absorber next to the gain section in a laser cavity introduces rich dynamics such as excitability, also observed in biological neurons, due to the different carrier lifetimes in the gain and absorber sections [6]. From previous work it is well understood that such a device can be bistable and has three operation regimes: cw, self-pulsation or an excitable regime [6]–[8]. In the two latter operation regimes spikes can be generated. Due to bistability, this device exhibits a hysteresis in the L-I characteristics and a negative differential resistance in the saturable absorber [8]. When the device is biased close to but below the hysteresis, an excitable response is expected when a perturbation above a threshold is applied [5]. Such non-linear response is the basic functionality of a neuron. Here, we demonstrate the bistability (i.e. the hysteresis and negative differential resistance) of an integrated two-section laser, fabricated in a multi-project wafer (MPW) InP platform, by measuring its L-I characteristics and the saturable absorber I-V curve. We also show how this laser exhibits noise-triggered self-spiking output (i.e., without any intentionally applied optical perturbation) with voltage controlled relative spike densities. We believe the self-spiking output could be useful to implement a rate-based encoding scheme in the input layer of an SNN, where the input data in such a network is translated to a spike density.

DEVICE AND EXPERIMENTAL SETUP

To experimentally observe a pulsed laser output, we fabricated two-section lasers, each consisting of a gain and a saturable absorber section on a commercial active-passive generic integration platform on InP [9]. Due to the maturity of this platform and the use of generic building blocks, future upscaling to an SNN containing multiple neurons is feasible. The device under investigation is a linear Fabry-Pérot type laser, comprising an 80 µm saturable absorber (SA) and 500 µm gain element (SOA), a 350 µm distributed Bragg reflector (DBR) optimized for reflections at 1550 nm, and a multimode interference reflector (MIR) (see the top laser in Fig. 1 (a)). The measurement setup for optical and electrical characterization is schematically shown in Fig. 1 (b). Light is coupled out of the chip using a lensed fiber coupler, and amplified using a low-noise EDFA. An optical isolator prevents reflections from the measurement equipment to interfere with the laser dynamics. An ILX Lightwave 3900 controller was used to pump

the gain section with current. To collect time traces a 6 GHz LeCroy Wavemaster 8600A real time oscilloscope was used.

Figure 1: (a) Micrograph of the fabricated PIC showing three lasers with different gain section lengths. (b) Overview of the measurement setup used to characterize the fabricated PIC. SMU: source measure unit, RTS: real time oscilloscope, PD: photodiode, PM: powermeter, EDFA: amplifier, ISO: optical isolator.

EXPERIMENTAL RESULTS

As mentioned in the introduction, the saturable absorber makes our two-section laser a bistable device. This bistability is experimentally confirmed by measuring the laser L-I and saturable absorber I-V characteristics, as shown in Fig. 2 (a) and (b). In case (a), a small positive current was applied to the saturable absorber to decrease the absorption. When the gain pump current is swept from 0 to 100 mA, denoted by the blue curve, a sudden stepwise increase of the optical output is seen at approximately 60 mA. By sweeping the gain current in the reverse direction, this step shifted to a lower current by approximately 10 mA. From similar measurements it was observed that this hysteresis width and step height can be tuned by changing the absorber current. In case (b), a negative differential resistance in the saturable absorber observed in the I-V characteristics. In this experiment, the gain section was first pumped at a relatively low current of 35 mA. The voltage at the saturable absorber was then swept from 0.0 to 1.0 V in steps of 0.01 V, while the current through the saturable absorber was monitored. This procedure was repeated for 10 different gain pump currents. At a saturable absorber voltage of 0 V, the absorption is strong and stimulated emission in the cavity is suppressed. Increasing the saturable absorber voltage decreases the absorption, which increases stimulated emission and the photon density in the cavity and as a results a larger negative photo current in the absorber is generated. This is observed in Fig. 2 (b) between approximately 0.5 V and 0.8 V for gain currents between 35 and 70 mA. In this case, the saturable absorber is bleached and the laser is turned on. When the voltage is further increased to a value above 0.8 V, the typical exponential diode characteristic becomes dominant [8].

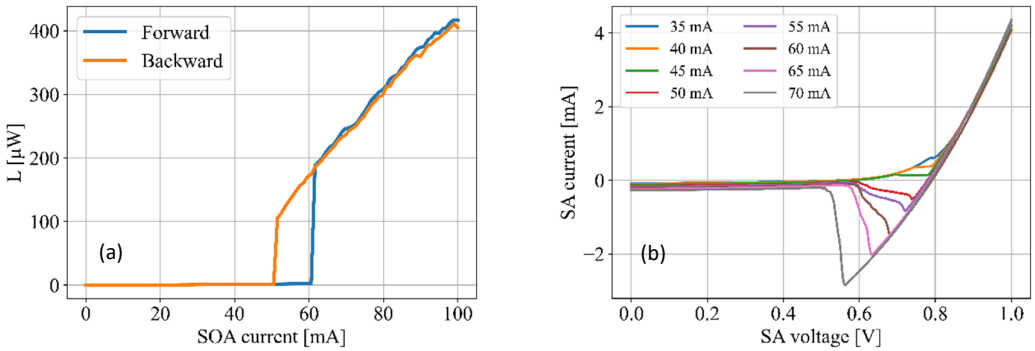

Figure 2: (a) Measured L-I laser characteristics for a small current applied at the saturable absorber. (b) Measured I-V saturable absorber characteristics for different gain currents as indicated.

In the next experiment, the gain section is biased at 50.11 mA, very close but slightly below the hysteresis. The optical output is analysed over 50 ms using the real time oscilloscope for three saturable absorber voltages, which are all located in the region of negative differential resistance shown in Fig. 2 (b). Fig. 3 (a), (b), and (c) show the oscilloscope time traces in case of a saturable absorber voltage of 0.720, 0.727, and 0.730 V, respectively. For all biasing conditions, pulses are observed in the time traces although the pulse densities are different. Note that in (b) and (c) the pulses do not show a fixed repetition rate, which would be expected for pulses generated in the self-pulsating operating regime. From this and given that the timescale is in the order of milliseconds, we conclude the observed pulses are not generated by the self-pulsating mechanism and relaxation oscillations but that these pulses likely are triggered by external noise. Note that because of the limited bandwidth of the real time oscilloscope, the temporal pulse width cannot be extracted from these time traces. However, as the generation of the pulses is directly related to the absorber and gain carrier lifetimes, which are in the order of hundreds and tens of picoseconds for this platform [10], we expect a sub-nanosecond pulse width.

SIMULATIONS

From previous numerical simulations, it was shown that in the region of excitability, injected noise can be strong enough to excite the laser and produce a pulse train [11]. To verify that the pulses in our experiment originate from injected noise, we simulated the two section laser using the normalized Yamada rate equations in the excitable regime [2]. This model describes the gain, absorber and optical intensity dynamics of a two section laser, where we added an extra term in the intensity equation to account for injected noise. We found that under reasonable normalized noise levels, the noise is indeed strong enough to perturb the laser and produce pulses. Similar to our experimental observations, the simulated pulse density increases when the absorption decreases.

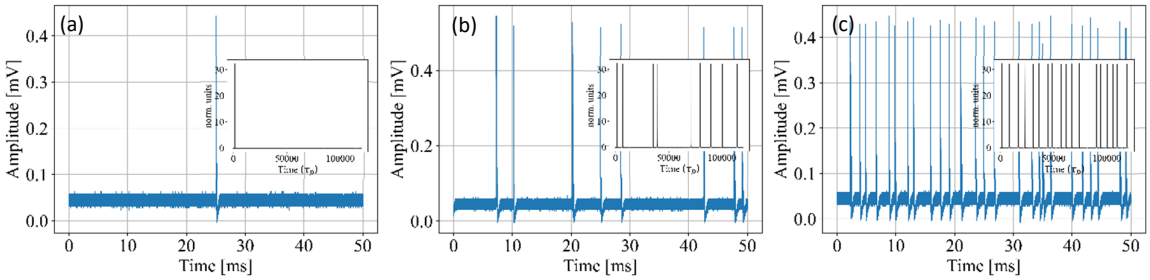

Figure 3: Time traces showing different pulse densities for V_{SA} = 0.720 V, 0.727 V, and 0.730 V, respectively. The gain section was pumped with a current of 50.11 mA. The insets show examples of the noise simulations with similar pulse densities.

CONCLUSION

We demonstrated bistability and voltage-dependent pulse densities when a two-section laser is biased close to this bistability. Simulations show that these pulses do not originate from self-pulsating mechanisms, but are likely triggered by external noise. We believe this is a successful first step towards a photonic SNN in an InP technology platform, since the proposed design can be used to encode data by controlling the pulse densities. Future work is aimed at achieving excitable pulse behaviour in the proposed structure, and realization of an all-optical photonic neuron as building block of a photonic SNN.

ACKNOWLEDGEMENT

We would like to thank Ruud van Sloun and Lizeth Gonzalez Carabarin for discussing the measurement results.

REFERENCES

[1] C. Huang *et al.*, “Prospects and applications of photonic neural networks,” *ArXiv210509943 Phys.*, May 2021, Accessed: Aug. 25, 2021. [Online]. Available: http://arxiv.org/abs/2105.09943

[2] M. A. Nahmias, B. J. Shastri, A. N. Tait, and P. R. Prucnal, “A Leaky Integrate-and-Fire Laser Neuron for Ultrafast Cognitive Computing,” *IEEE J. Sel. Top. Quantum Electron.*, vol. 19, no. 5, pp. 1–12, Sep. 2013, doi: 10.1109/JSTQE.2013.2257700.

[3] M. Hejda, J. Robertson, J. Bueno, J. A. Alanis, and A. Hurtado, “Neuromorphic encoding of image pixel data into rate-coded optical spike trains with a photonic VCSEL-neuron,” *APL Photonics*, vol. 6, no. 6, p. 060802, Jun. 2021, doi: 10.1063/5.0048674.

[4] Y. Zhang, J. Robertson, S. Xiang, M. Hejda, J. Bueno, and A. Hurtado, “All-optical neuromorphic binary convolution with a spiking VCSEL neuron for image gradient magnitudes,” *Photonics Res.*, vol. 9, no. 5, p. B201, May 2021, doi: 10.1364/PRJ.412141.

[5] R. Otupiri, B. Garbin, N. G. R. Broderick, and B. Krauskopf, “Excitability in an all-fiber laser with a saturable absorber section,” *J. Opt. Soc. Am. B*, vol. 38, no. 5, p. 1695, May 2021, doi: 10.1364/JOSAB.420204.

[6] R. Otupiri, B. Krauskopf, and N. G. R. Broderick, “The Yamada model for a self-pulsing laser: bifurcation structure for non-identical decay times of gain and absorber,” *Int. J. Bifurc. Chaos*, vol. 30, no. 14, p. 2030039, Nov. 2020, doi: 10.1142/S0218127420300396.

[7] L. Puts, W. Yao, and D. Lenstra, “Modeling a Spiking Optical Neuron using Normalized Yamada Rate Equations,” in *25th Annual Symposium of the IEEE Photonics Benelux*, Mons, Belgium, Nov. 2021, p. 4.

[8] C. Harder, Kam Lau, and A. Yariv, “Bistability and pulsations in semiconductor lasers with inhomogeneous current injection,” *IEEE J. Quantum Electron.*, vol. 18, no. 9, pp. 1351–1361, Sep. 1982, doi: 10.1109/JQE.1982.1071711.

[9] M. Smit *et al.*, “An introduction to InP-based generic integration technology,” *Semicond. Sci. Technol.*, vol. 29, no. 8, p. 083001, Jun. 2014, doi: 10.1088/0268-1242/29/8/083001.

[10] V. Moskalenko, *Extended cavity passively mode-locked lasers in indium phosphide generic integration technology*. Technische Universiteit Eindhoven, 2016.

[11] J. L. A. Dubbeldam, B. Krauskopf, and D. Lenstra, “Excitability and coherence resonance in lasers with saturable absorber,” *Phys. Rev. E*, vol. 60, no. 6, pp. 6580–6588, Dec. 1999, doi: 10.1103/PhysRevE.60.6580.